Supersensitivity in a chain of closely spaced electric dipoles with variable moments

Evgeniy G. Fateev*
Institute of Applied Mechanics, Ural Division, Russian Academy of Sciences, Izhevsk 426000, Russia
(Received 13 June 2001; published 14 January 2002)

A chain of closely spaced oscillators is studied theoretically. The oscillators are interrelated electric dipoles whose moments may vary within a wide range. An expression for the oscillator interaction potential is suggested. On the basis of this potential, a one-dimensional nonlinear equation of motion is derived with allowance made for dissipation and external driving. A numerical investigation is carried out, and various nonlinear phenomena are revealed in the chain. Among them are the size effect and ultrasensitivity, i.e., a giant response of the chain to extremely weak periodic perturbations. The findings are compared with previously obtained experimental results on naturally occurring objects with similar structure. It is inferred that the model is realistic.

DOI: 10.1103/PhysRevE.65.021403 PACS number(s): 82.70.−y, 05.45.Ra, 77.22.−d, 87.10.+e

I. INTRODUCTION

This paper deals with a system of closely spaced oscillating electric dipoles with variable and interrelated dipole moments in the presence of dissipation and perturbation. It is a challenging problem to ascertain the behavior of the system even in a one-dimensional case. In practical terms, this model may provide valuable insight into remarkable phenomena in some types of heterogeneous condensed media that has been exposed to an electromagnetic field of an ultralow frequency (ULF) below 10^3 Hz. The medium consists of a nonconducting or semiconducting continuous phase and inclusions with liquid or quasiliquid conducting sheaths. Such structures are usually formed in almost any insulator during a phase transition. They permanently exist in powders and water-saturated rock. They are also basically similar to certain systems of cells in organisms. A realistic model of such media should take into account the close spacing of the oscillators and the variation in their dipole moments. Otherwise, many interesting phenomena may be overlooked.

Among the phenomena is the ultrasensitivity of crystalline hydrates to ULF under strong compression. This recently detected effect manifests itself in the giant mechanical response to an extremely weak electric field in a very narrow ULF range where the field strength is lower than the electric breakdown threshold by a factor of about $\sim 10^3$ [1]. Furthermore, the frequency range shifts if the medium is heated [2]. The effect is preceded by giant bursts of dielectric susceptibility at ULFs, which apparently result from the formation of short-lived heterogeneous structures, including nonconducting microinclusions with thin liquid sheaths containing mobile ions. Susceptibility bursts in such media experiencing ULF fields have been reported by many researchers (see the references in [3]). The phenomenon stems mainly from the accumulation of extremely large amounts of polarization charges (free anions or cations) at the poles of the microinclusions so that the dipole moments of the oscillators change considerably. However, in contrast to dielectric-loss spectra, the reported shapes of ULF permittivity have no narrow or wide peaks at any moment of growth. They are smooth curves obeying the Debye-spectrum dispersion relation. The point is that dipole-dipole interaction in the chain has been neglected when dealing with inhomogeneous media in ULF fields because of computational difficulties. Accordingly, attempts to relate the giant susceptibility bursts at ULFs to the giant mechanical response resulted in rather academic models of gas breakdown in microcracks of crystalline-hydrate plates under compression. The models imply that a ULF peak may arise in input-power spectral density, which leads to a singularity in the ultrasensitivity spectrum [3]. The peak would be noticeable if the charge relaxation time τ of the sheaths was about $\sim 10^{-2}$ s and the particle size was in the micrometer range. In reality, $\tau = 1/\Omega \sim 10^{-5}$ s, where $\Omega \sim 5 \times 10^4$ Hz is the frequency corresponding to the maximum in dielectric loss. Furthermore, the models state that a ULF peak arises only if each physical property of the gas in microcracks is within a very narrow range. The above considerations have led us to the conclusion that a chain of closely spaced oscillating dipoles with variable moments should be used as a physical model of ultrasensitivity. In particular, this approach could help one understand why the phenomenon is confined to a narrow ULF range, at least at the onset of excitation.

To explain the above phenomena, a one-dimensional chain of closely spaced oscillating electric dipoles is considered, with a and $2r$ standing for the average dipole spacing and the charge spacing of a dipole, respectively (Fig. 1). Based on this model, the total potential of the interaction between the oscillators should be determined and the system behavior under the action of an ULF electric field should be investigated. Recall that well-known models based on oscillator chains with nonlinear coupling typically imply that the dipole moments are constant and $a \gg 2r$ [4–7]. Although this approach works well with certain quasi-one-dimensional chains, it fails when applied to various systems where dipole charges vary by one to four orders of magnitude, depending on the oscillator spacing, oscillator natural frequencies, etc. Accordingly, this study follows the course outlined in this section. Also, we compare the computed behavior of the chain with experimental data.

The structure of this paper is the following. In Sec. II, the

*Email addresses: fateev@ipm.uni.udm.ru and e@fateev.udm.ru

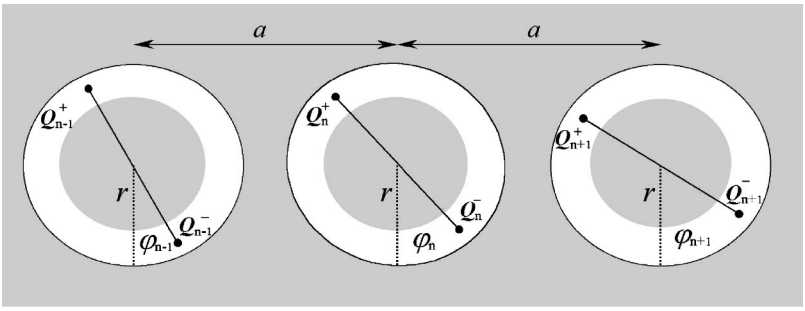

FIG. 1. Configuration of the dipole-oscillator chain ($n=1,2,...,N$) with spacing a. Each oscillator represents a particle of diameter $2r$ with a sheath containing oscillating charges. The sheath thickness may be ~30–300Å.

model describing the interaction between closely spaced dipoles in a chain with strongly variable moments is given. Solving the Euler-Lagrange equation with the help of the corresponding potential of interaction, we find the nonlinear equation of motion in this system. In Sec III, the actual order of certain coefficients for this equation is evaluated. In Sec. IV, the results of the numerical computations are given. The existence of the dependence of the value of the maximal level of polarization in the dipole chain with variable moments on the quantity of dipoles in the chain is demonstrated. It is shown that this size effect results in the possibility of supersensitivity in these chains or strong polarization at least in one dipole oscillator in the chain when the entire chain is excited by ultra-weak electromagnetic signals at ultralow frequencies. In Sec. V, the results of the computations are discussed. In the final part, the conclusions are given.

II. MODEL DESCRIPTION

The model is illustrated in Fig. 1. The potential energy will be calculated for the case of $a \gg 2r$, where a is the average oscillator spacing and r is the oscillator radius with variable dipole moments. Thus, neighboring oscillators may be in contact. Furthermore, we assume that the polarization level may be very sensitive to both the frequencies and the strengths of local and external fields. Dipole-dipole interaction will be treated in the Coulomb approximation. For the respective oscillators, let φ_{n-1}, φ_n, and φ_{n+1} denote the deflection angles of the dipole axes from the unstable-equilibrium positions (Fig. 1). Then, the potential energy of the oscillator system has the general form

$$U_{\rm int}=\frac{1}{4\pi\varepsilon\varepsilon_o}\sum_n\left\{\left(\frac{Q^+_{n-1}Q^+_n\mathbf{R}^{++}_{n-1,n}}{(R^{++}_{n-1,n})^2}+\frac{Q^-_{n-1}Q^-_n\mathbf{R}^{--}_{n-1,n}}{(R^{--}_{n-1,n})^2}-\frac{Q^-_{n-1}Q^+_n\mathbf{R}^{-+}_{n-1,n}}{(R^{-+}_{n-1,n})^2}-\frac{Q^+_{n-1}Q^-_n\mathbf{R}^{+-}_{n-1,n}}{(R^{+-}_{n-1,n})^2}\right)+\left(\frac{Q^+_nQ^+_{n+1}\mathbf{R}^{++}_{n,n+1}}{(R^{++}_{n,n+1})^2}+\frac{Q^-_nQ^-_{n+1}\mathbf{R}^{--}_{n,n+1}}{(R^{--}_{n,n+1})^2}-\frac{Q^-_nQ^+_{n+1}\mathbf{R}^{-+}_{n,n+1}}{(R^{-+}_{n,n+1})^2}-\frac{Q^+_nQ^-_{n+1}\mathbf{R}^{+-}_{n,n+1}}{(R^{+-}_{n,n+1})^2}\right)\right\}. \quad (1)$$

Here, the distances between the charges of the $(n-1)$th dipole and those of the nth dipole are expressed as

$$R^{++}_{n-1,n}=[\{a-r(\sin\varphi_{n-1}-\sin\varphi_n)\}^2+r^2(\cos\varphi_{n-1}-\cos\varphi_n)^2]^{1/2}=\left\{a^2+4r\sin\left(\frac{\varphi_n-\varphi_{n-1}}{2}\right)\left[r\sin\left(\frac{\varphi_n-\varphi_{n-1}}{2}\right)+a\cos\left(\frac{\varphi_n+\varphi_{n-1}}{2}\right)\right]\right\}^{1/2}, \quad (2)$$

$$R^{--}_{n-1,n}=\{[a+r(\sin\varphi_{n-1}-\sin\varphi_n)]^2+r^2(\cos\varphi_{n-1}-\cos\varphi_n)^2\}^{1/2}=\left\{a^2+4r\sin\left(\frac{\varphi_n-\varphi_{n-1}}{2}\right)\left[r\sin\left(\frac{\varphi_n-\varphi_{n-1}}{2}\right)-a\cos\left(\frac{\varphi_n+\varphi_{n-1}}{2}\right)\right]\right\}^{1/2}, \quad (3)$$

$$R^{-+}_{n-1,n}=\{[a+r(\sin\varphi_{n-1}+\sin\varphi_n)]^2+r^2(\cos\varphi_{n-1}+\cos\varphi_n)^2\}^{1/2}=\left\{a^2+4r\cos\left(\frac{\varphi_n-\varphi_{n-1}}{2}\right)\left[r\cos\left(\frac{\varphi_n-\varphi_{n-1}}{2}\right)+a\sin\left(\frac{\varphi_n+\varphi_{n-1}}{2}\right)\right]\right\}^{1/2}, \quad (4)$$

$$R^{+-}_{n-1,n}=\{[a-r(\sin\varphi_{n-1}+\sin\varphi_n)]^2+r^2(\cos\varphi_{n-1}+\cos\varphi_n)^2\}^{1/2}=\left\{a^2+4r\cos\left(\frac{\varphi_n-\varphi_{n-1}}{2}\right)\left[r\cos\left(\frac{\varphi_n-\varphi_{n-1}}{2}\right)-a\sin\left(\frac{\varphi_n+\varphi_{n-1}}{2}\right)\right]\right\}^{1/2}. \quad (5)$$

In Eq. (1) $\mathbf{R}^{++}_{n-1,n}$, $\mathbf{R}^{--}_{n-1,n}$, $\mathbf{R}^{-+}_{n-1,n}$, $\mathbf{R}^{+-}_{n-1,n}$, $\mathbf{R}^{++}_{n,n+1}$, $\mathbf{R}^{--}_{n,n+1}$, $\mathbf{R}^{-+}_{n,n+1}$, $\mathbf{R}^{+-}_{n,n+1}$, denote the radius vectors between the respective charges in the chain. The respective distances $R^{++}_{n,n+1}$, $R^{--}_{n,n+1}$, $R^{-+}_{n,n+1}$, and $R^{+-}_{n,n+1}$ between the charges Q^+_{n+1}, Q^-_{n+1}, Q^+_n, and Q^-_n in dipoles $n+1$ and n obey formulas that can be derived from Eqs. (2)–(5) by replacing n with $n+1$ and $n-1$ with n. Finally, ε is the relative permittivity of the medium and ε_o is the permittivity of free space. It is convenient to recast Eq. (1) as

$$U_{\rm int}=\frac{1}{4\pi\varepsilon\varepsilon_o}\sum_n\left\{Q_n^+\left(\frac{Q_n^+\mathbf{R}_{n-1,n}^{++}}{(R_{n-1,n}^{++})^2}-\frac{Q_n^+\mathbf{R}_{n,n+1}^{++}}{(R_{n,n+1}^{++})^2}\right)+Q_n^-\left(\frac{Q_{n-1}^-\mathbf{R}_{n-1,n}^{--}}{(R_{n-1,n}^{--})^2}-\frac{Q_{n+1}^-\mathbf{R}_{n,n+1}^{--}}{(R_{n,n+1}^{--})^2}\right)+Q_n^+\left(\frac{Q_{n+1}^-\mathbf{R}_{n,n+1}^{-+}}{(R_{n,n+1}^{-+})^2}-\frac{Q_{n-1}^-\mathbf{R}_{n-1,n}^{-+}}{(R_{n-1,n}^{-+})^2}\right)+Q_n^-\left(\frac{Q_{n+1}^+\mathbf{R}_{n,n+1}^{+-}}{(R_{n,n+1}^{+-})^2}-\frac{Q_{n-1}^+\mathbf{R}_{n,n+1}^{+-}}{(R_{n,n+1}^{+-})^2}\right)\right\}. \tag{6}$$

Now, let us take into account that the charge of dipole n depends on external and local electric fields, the latter being produced by the moving charges of dipoles $n-1$ and $n+1$. Assume that the other dipoles act on dipole n only indirectly via the chain as a result of shielding. We neglect other physical and chemical processes in the oscillators and around them that may affect polarization (for details, see [9–11]). The contribution of external and local fields to the polarization of any of the charges Q_n^+, Q_n^-, Q_{n-1}^+, and Q_{n-1}^- is assumed to obey the superposition principle, allowing for the frequency dependence. For any oscillator, the frequencies of the positive and the negative charges are considered to be the same. For each oscillator, let the dependence of the polarization on the frequencies of the local and the external field ω_n and Ω, respectively, obey the Debye dispersion law [9,10]. Since ($|Q_n^+|=|Q_n^-|$), the respective dipole charges of the $(n-1)$th, nth, and $(n+1)$th oscillators are expressed as

$$Q_n^+=\beta\left\{\frac{c_o e(\varepsilon_s-\varepsilon_\infty)\mathbf{R}_{n,n-1}^{++}}{4\pi\varepsilon\varepsilon_o[1+(\tau\omega_{n-1})^2](R_{n,n-1}^{++})^3}+\frac{c_o e(\varepsilon_s-\varepsilon_\infty)\mathbf{R}_{n,n+1}^{++}}{4\pi\varepsilon\varepsilon_o[1+(\tau\omega_{n+1})^2](R_{n,n+1}^{++})^3}-\frac{c_o e(\varepsilon_s-\varepsilon_\infty)\mathbf{R}_{n,n-1}^{-+}}{4\pi\varepsilon\varepsilon_o[1+(\tau\omega_{n-1})^2](R_{n,n-1}^{-+})^3}-\frac{c_o e(\varepsilon_s-\varepsilon_\infty)\mathbf{R}_{n,n+1}^{+-}}{4\pi\varepsilon\varepsilon_o[1+(\tau\omega_{n+1})^2](R_{n,n+1}^{+-})^3}+\frac{E_n^{\rm ext}}{1+(\tau\Omega)^2}\right\}, \tag{7}$$

$$Q_{n-1}^+=\beta\left\{\frac{c_o e(\varepsilon_s-\varepsilon_\infty)\mathbf{R}_{n-1,n-2}^{++}}{4\pi\varepsilon\varepsilon_o[1+(\tau\omega_{n-2})^2](R_{n-1,n-2}^{++})^3}+\frac{c_o e(\varepsilon_s-\varepsilon_\infty)\mathbf{R}_{n-1,n}^{++}}{4\pi\varepsilon\varepsilon_o[1+(\tau\omega_n)^2](R_{n-1,n}^{++})^3}-\frac{c_o e(\varepsilon_s-\varepsilon_\infty)\mathbf{R}_{n-1,n-2}^{-+}}{4\pi\varepsilon\varepsilon_o[1+(\tau\omega_{n-2})^2](R_{n-1,n-2}^{-+})^3}-\frac{c_o e(\varepsilon_s-\varepsilon_\infty)\mathbf{R}_{n-1,n}^{+-}}{4\pi\varepsilon\varepsilon_o[1+(\tau\omega_n)^2](R_{n-1,n}^{+-})^3}+\frac{E_{n-1}^{\rm ext}}{1+(\tau\Omega)^2}\right\}, \tag{8}$$

$$Q_{n+1}^+=\beta\left\{\frac{c_o e(\varepsilon_s-\varepsilon_\infty)\mathbf{R}_{n+1,n}^{++}}{4\pi\varepsilon\varepsilon_o[1+(\tau\omega_n)^2](R_{n+1,n}^{++})^3}+\frac{c_o e(\varepsilon_s-\varepsilon_\infty)\mathbf{R}_{n+1,n+2}^{++}}{4\pi\varepsilon\varepsilon_o[1+(\tau\omega_{n+2})^2](R_{n+1,n+2}^{++})^3}-\frac{c_o e(\varepsilon_s-\varepsilon_\infty)\mathbf{R}_{n+1,n}^{-+}}{4\pi\varepsilon\varepsilon_o[1+(\tau\omega_n)^2](R_{n+1,n}^{-+})^3}\times\frac{c_o e(\varepsilon_s-\varepsilon_\infty)\mathbf{R}_{n+1,n+2}^{+-}}{4\pi\varepsilon\varepsilon_o[1+(\tau\omega_{n+2})^2](R_{n+1,n+2}^{+-})^3}+\frac{E_{n+1}^{\rm ext}}{1+(\tau\Omega)^2}\right\}, \tag{9}$$

where τ is the relaxation time of bound charges in sheaths and ε_s and ε_∞ are the maximum static low frequency (SLF) and the minimum high-frequency (optical) values of the permittivity, respectively.

The coefficient c_o is the number of elementary dipole charges e that change the permittivity of the system by unity during polarization. Let the chain be subjected to a uniform harmonic external field directed along the chain axis. In the vicinity of an nth oscillator, the field is expressed as

$$E_n^{\rm ext}=2\varepsilon^{-1}E\sin(2\pi\Omega t)\cos(\varphi_n). \tag{10}$$

Similar expressions describe the field near oscillators $n-1$ and $n+1$. To evaluate E_n, E_{n-1}, and E_{n+1} we assume that the charge of dipole n or $n-1$ tends to $Q_\infty=c_o e\varepsilon_\infty$ for $\omega_n\to\infty$ and to $Q_o=c_o(\varepsilon_s-\varepsilon_\infty)$ for $\omega_n\to 0$. Also, we assume that $c_o=$const for each oscillator in the chain. The coefficient β corresponds to the dipole charge that is induced in a field of unit strength. In other words, β specifies the polarization susceptibility of an oscillator. It is similar to dielectric susceptibility, which represents the relationship between the polarization and the field strength in a macroscopic dielectric body. To a first approximation, we regard β as a constant here. In reality, it may depend on many other parameters.

Let us assume that the variables φ_n are nearly identical for neighboring dipoles at the same point in time. Accordingly, if we perform the change $na\to x$ and $\varphi_n(t)\to\varphi(x,t)$ in the continuum approximation $\varphi_n-\varphi_{n-1}\sim\delta$, then $U_{\rm int}$ can be expanded in terms of a small parameter as

$$\varphi_n-\varphi_{n-1}\simeq\varphi_{n+1}-\varphi_n\sim a\frac{\partial\varphi}{\partial x}. \tag{11}$$

In view of Eqs. (1)–(11) and the accompanying comments, we obtain an expression for $U_{\rm int}$ by passing to the limit for $a\to 2r+\Delta$ in the expansion to second-order terms. In the continuum approximation, it can be written as

$$U_{\rm int}=\frac{1}{4\pi\varepsilon\varepsilon_o}\int\frac{\partial x}{a}\beta^2V_1(x,t)V_2(x,t)\times\Big\{-[P(t)\cos(\varphi)+B(x,t)V_3(x,t)]-B(x,t)[P(t)\cos(\varphi)V_4(x,t)+V_3(x,t)V_5(x,t)]\frac{\partial\varphi}{\partial x}-B(x,t)[5P(t)\cos(\varphi)\{V_6(x,t)+V_7(x,t)\}+9V_3(x,t)V_7(x,t)]\Big\},\tag{12}$$

with

$$P(t)=\frac{2E\sin(2\pi\Omega t)}{\varepsilon[1+(\tau\Omega)^2]}.\tag{13}$$

$$S_1(x,t)=a^2+4r^2-4ra\sin(\varphi),\tag{14}$$

$$S_2(x,t)=a^2+4r^2+4ra\sin(\varphi),\tag{15}$$

$$B(x,t)=\frac{c_oe(\varepsilon_s-\varepsilon_\infty)}{4\pi\varepsilon\varepsilon_o[1+(\tau\varphi_t)^2]},\tag{16}$$

$$V_1(x,t)=P(t)\cos(\varphi)+B(x,t)[S_1^{-1}(x,t)-S_2^{-1}(x,t)],\tag{17}$$

$$V_2(x,t)=S_1^{-1/2}(x,t)+S_2^{-1/2}(x,t),\tag{18}$$

$$V_3(x,t)=S_1^{-1}(x,t)+S_2^{-1}(x,t),\tag{19}$$

$$V_4(x,t)=4ra^2\cos(\varphi)[S_1^{-2}(x,t)+S_2^{-2}(x,t)],\tag{20}$$

$$V_5(x,t)=-ra^2\cos(\varphi)B(x,t)S_1^{-1}(x,t),\tag{21}$$

$$V_6(x,t)=2ra^3\sin(\varphi)S_2^{-2}(x,t)+4r^2a^4\cos^2(\varphi)S_2^{-3}(x,t),\tag{22}$$

$$V_7(x,t)=-2ra^3\sin(\varphi)S_1^{-2}(x,t)+4r^2a^4\cos^2(\varphi)S_1^{-3}(x,t).\tag{23}$$

When deriving Eq. (12), formula (6) was used, because in the limit of $a\to2r+\Delta$, the first two summands in parentheses become negligible compared to the remainder. For the same reason, each of the formulas (7)–(9) was used without the first two summands that account for the interaction between like charges of neighboring dipoles. Obviously, this simplification is justified by the existence of potential wells at $\varphi_n=\pi/2+n\pi$, which become deeper as opposite charges of neighboring dipoles grow owing to polarization.

Let c_n denote the number of uncompensated charged particles (such as cations or anions) in the sheath of an nth oscillator so that the total mass of the charged particles at the ends of the nth dipole is $M_n=c_nm$, each particle having mass m. Then the kinetic energy of the chain is given by

$$T_k=\frac{1}{2}\sum_n J_n\left(\frac{\partial\varphi_n}{\partial t}\right)^2.\tag{24}$$

Here, $J_n=c_nmr^2$ is the moment of inertia. Furthermore, in view of Eq. (7)

$$c_n=Q_n^+/e.\tag{25}$$

In the continuum approximation, expansion to the second-order terms yields

$$T_k=\beta\frac{mr^2}{e}\int\frac{dx}{a}\left\{V_1(x,t)+B(x,t)V_8(x,t)\frac{\partial\varphi}{\partial x}+B(x,t)V_9(x,t)\frac{\partial^2\varphi}{\partial x^2}\right\}\left(\frac{\partial\varphi}{\partial t}\right)^2,\tag{26}$$

with

$$V_8(x,t)=6ra^2\cos(\varphi)S_1^{-2}(x,t),\tag{27}$$

$$V_9(x,t)=-5ra^3\sin(\varphi)S_1^{-2}(x,t)+36r^2a^4\cos^2(\varphi)S_1^{-3}(x,t).\tag{28}$$

Now, we assume that the dissipative forces are linear functions of charge angular velocities. Then, with ξ_n denoting the dissipation parameter, the dissipation has the form

$$D=\frac{1}{2}\sum_n c_n\xi_nr^2\left(\frac{\partial\varphi_n}{\partial t}\right)^2.\tag{29}$$

The above reasoning for the kinetic energy, including formulas (25) and (7), can be also applied to the dissipation function. In the continuum approximation, expansion to the second-order terms yields

$$D=\beta\frac{\xi r^2}{e}\int\frac{dx}{a}\left\{V_1(x,t)+B(x,t)V_8(x,t)\frac{\partial\varphi}{\partial x}+B(x,t)V_9(x,t)\frac{\partial^2\varphi}{\partial x^2}\right\}\left(\frac{\partial\varphi}{\partial t}\right)^2.\tag{30}$$

The force with which the external field acts on the chain can be expressed as

$$F=2\varepsilon^{-1}E\sin(2\pi\Omega t)\sum_n Q_n\cos(\varphi_n).\tag{31}$$

where Q_n addictively depends on local and external fields, according to Eq. (7). Let us expand F into a series. By analogy with Eqs. (26) and (30), the continuum approximation yields

$$F=2\varepsilon^{-1}E\sin(2\pi\Omega t)\int\frac{dx}{a}\cos(\varphi)\left\{V_1(x,t)+B(x,t)V_8(x,t)\frac{\partial\varphi}{\partial x}+B(x,t)V_9(x,t)\frac{\partial^2\varphi}{\partial x^2}\right\}.\tag{32}$$

It follows from expressions (11) and (30) that the effective force applied to the chain is proportional to the squared amplitude of the external ac field. Now, let us write the Euler-Lagrange equation with regard for dissipation (30) and perturbation

$$\frac{\partial\varphi}{\partial t}\left(\frac{\partial L}{\partial\varphi_t}\right)+\frac{\partial\varphi}{\partial x}\left(\frac{\partial L}{\partial\varphi_x}\right)-\frac{\partial L}{\partial\varphi}=-\frac{\partial D}{\partial\varphi_t}+F(x,t). \quad (33)$$

Here, the Lagrangian

$$L=T_k-U_{\rm int} \quad (34)$$

involves formulas (26) and (12) for the potential and kinetic energies, respectively. In the continuum approximation, Eq. (33) can be transformed into the following nonlinear motion equation written in natural units

$$W_1\frac{\partial^2\varphi}{\partial t^2}+W_2+X_1\frac{\partial^2\varphi}{\partial x^2}+X_2-\Gamma_1\sin(\varphi)-\Gamma_2+{\rm Dis}\frac{\partial\varphi}{\partial t}=F. \quad (35)$$

When deriving Eq. (35), for each differentiation, we neglected the terms with $1/a$ raised to the minimum power. This simplification is based on the assumption that $a\ll 1$ in natural units. Introducing the notation

$$\varphi_t=\frac{\partial\varphi}{\partial t},\quad \varphi_x=\frac{\partial\varphi}{\partial x},\quad \varphi_{xt}=\frac{\partial^2\varphi}{\partial x\partial t},\quad \varphi_{xx}=\frac{\partial^2\varphi}{\partial x^2},$$

we write expressions for the functions appearing in Eq. (35) as

$$W_1(x,t)=2MV_1(x,t)+2V_2(x,t)V_{11}(x,t)\times\left[V_1(x,t)V_3(x,t)+V_{10}(x,t)\left(\frac{\partial\varphi}{\partial x}\right)^2\right], \quad (36)$$

$$W_2(x,t)=2M\tfrac{\partial}{\partial t}V_1(x,t)\tfrac{\partial\varphi}{\partial t}+2\beta^2V_2(x,t)\tfrac{\partial}{\partial t}B(x,t)\times\left\{V_3(x,t)\tfrac{\partial}{\partial t}V_1(x,t)+V_1(x,t)\tfrac{\partial}{\partial t}V_3(x,t)+\frac{\partial}{\partial t}V_{10}(x,t)\left(\frac{\partial\varphi}{\partial x}\right)^2+2V_{10}(x,t)\left(\frac{\partial\varphi}{\partial x}\right)\frac{\partial^2\varphi}{\partial t\partial x}\right\}, \quad (37)$$

where

$$V_{10}(x,t)=5P(t)\cos(\varphi)[V_6(x,t)+V_7(x,t)]+9V_3(x,t)V_7(x,t), \quad (38)$$

$$V_{11}(x,t)=\frac{2A\chi\tau^2}{[1+(\tau\varphi_t)^2]^2}\left\{\frac{4(\tau\varphi t)^2}{1+(\tau\varphi_t)^2}-1\right\}. \quad (39)$$

$$A=c_oe(\varepsilon_s-\varepsilon_\infty),\quad \chi=\frac{1}{4\pi\varepsilon\varepsilon_o},\quad M=\frac{mr^2}{2e}. \quad (40)$$

Also, we have,

$$\Gamma_1(x,t)=M\sin^{-1}(\varphi)[V_{13}(x,t)+48r^2a^3MB(x,t)\times\cos^2(\varphi)S_1^{-3}(x,t)\varphi_x]\left(\frac{\partial\varphi}{\partial t}\right)^2+12\sin(\varphi)\beta^2V_1(x,t)V_{12}(x,t)[P(t)\cos(\varphi)+B(x,t)V_3(x,t)],\quad \Gamma_2(x,t)=0, \quad (41)$$

where

$$V_{12}(x,t)=2ra\cos(\varphi)[S_1^{-3/2}(x,t)-S_2^{-3/2}(x,t)], \quad (42)$$

$$V_{13}(x,t)=-P(t)\sin(\varphi)+4raA\chi\times\cos(\varphi)[S_1^{-2}(x,t)-S_2{}^{-2}(x,t)]. \quad (43)$$

In addition,

$$X_1(x,t)=2MB(x,t)V_9(x,t)\varphi_t^2+2\beta^2P(t)V_2(x,t)\times\{5\cos(\varphi)[V_6(x,t)+V_7(x,t)]+9V_8(x,t)V_7(x,t)\}, \quad (44)$$

$$X_2(x,t)=MB(x,t)\tfrac{\partial}{\partial x}V_8(x,t)\varphi_t^2+2MB(x,t)\tfrac{\partial}{\partial x}V_9(x,t)\varphi_t^2\varphi_x+A\beta^2V_2(x,t)\{2V_5(x,t)\tfrac{\partial}{\partial x}V_3(x,t)+2V_3(x,t)\tfrac{\partial}{\partial x}V_5(x,t)-P(t)\sin(\varphi)V_4(x,t)\varphi_x\}+18A\beta^2V_2(x,t)\{V_7(x,t)\tfrac{\partial}{\partial x}V_3(x,t)+V_3(x,t)\tfrac{\partial}{\partial x}V_7(x,t)\}\varphi_x. \quad (45)$$

Finally,

$${\rm Dis}(x,t)=2\beta\Psi\{V_1(x,t)+B(x,t)[V_8(x,t)\varphi_x+V_9(x,t)\varphi_x^2]-B(x,t)(1+\tau^2\varphi_t^2)^{-1}V_8(x,t)\tau^2\varphi_t^2\varphi_x\}, \quad (46)$$

with

$$\Psi=\frac{\xi r^2}{2e}, \quad (47)$$

and

$$F(x,t)=2\varepsilon^{-1}E\beta\sin(2\pi\Omega t)\cos(\varphi)[V_1(x,t)+B(x,t)V_8(x,t)\varphi_x+B(x,t)V_9(x,t)\varphi_x^2]. \quad (48)$$

It is convenient to recast Eq. (35) in a form similar to the sine-Gordon (SG) equation

$$\frac{\partial^2\varphi}{\partial t^2}+v_o^2\frac{\partial^2\varphi}{\partial x^2}-\theta_o^2\sin(\varphi)-\eta\frac{\partial\varphi}{\partial t}=\gamma(x,t). \quad (49)$$

Here,

$$v_o=\sqrt{X_1(x,t)/W_1(x,t)}, \quad (50)$$

is an analog of the maximum velocity at which a perturbation propagates into the chain. Also,

$$\theta_o=\sqrt{\Gamma_1(x,t)/W_1(x,t)} \quad (51)$$

is an analog of the plasma frequency. In Eq. (49), the level of dissipation is represented by

$$\eta={\rm Dis}(x,t)/W_1(x,t), \quad (52)$$

and the perturbation, by

$$\gamma(x,t)=[F(x,t)-W_2(x,t)-X_2(x,t)+\Gamma_2(x,t)]/W_1(x,t). \tag{53}$$

With l denoting the length of the chain, we introduce the boundary condition

$$\varphi(0,t)=\varphi(l,t)=0. \tag{54}$$

Physically, condition (54) may correspond to an interphase boundary, which is impermeable to the perturbations under consideration.

III. ESTIMATIONS FOR THE COEFFICIENTS IN EQUATION (49)

Let us find the values for the coefficients in Eq. (49) so that the chain can simulate most closely the behavior of naturally occurring objects, such as disperse systems or long chains of living cells. To this end, let us estimate the number of uncompensated elementary charges in the thin liquid sheaths which determine the spherical shape of each oscillator (Fig. 1). We assume that a particle of the majority carrier has a charge $e\sim1.6\times10^{-19}$ C and a mass $m\sim1.6\times10^{-27}$ kg (its effective mass may be much larger). For example, such a carrier may be an H^+ ion, since its mobility is much higher than that of OH^- or other anions and cations. Let $r\sim10^{-6}-10^{-3}$ m and $a\sim3\times10^{-6}-3\times10^{-3}$ m. The sheath thickness d may be set at about $\sim10^{-9}-10^{-8}$ m [8]. We assume that at least $\chi_1\sim1\%$ of water in the sheaths is dissociated and that $\chi_2\sim1\%$ of the anions and cations constitute the uncompensated charges. Then the density of elementary charges that may be involved in polarization is estimated at

$$c_1=\chi_1\chi_2 4\pi[(r+d)^3-r^3]\rho_{H_2O}(3m)^{-1}$$
$$\sim10^{11}-10^{14}\ \text{charge/mm}^3, \tag{55}$$

where $\rho\sim10^3$ kg/m^3 is the water density and $m_{H_2O}\approx3\times10^{-27}$ is the mass of a water molecule.

Thus, we see that the above estimate of c_1 agrees with the well-known value of $\sim10^{11}$charge/mm^3 [8]. Correspondingly, $Q^+=c_1e$ is $\sim10^{-12}-10^{-9}$ C. Strictly speaking, the parameters should depend on the thermodynamic and local properties of the medium.

We select the value of c_1 such that the uncompensated charge Q is no larger than $10^{-12}-10^{-9}$ C when the polarization is at its maximum. The relaxation time is defined as $\tau_1=r^2/2D$, where D is the volume diffusion coefficient of charges in the sheaths. The relaxation time is evaluated from the frequency $\omega=1/\tau_1$ which corresponds to the highest dielectric loss. In the context of this study, $\omega\approx6.29\times10^4$ rad/s, so that $\tau\approx1.6\times10^{-5}$ s.

Finally, consider the case of a disperse system. For the nth dipole, the fraction of its kinetic energy (apart from thermal fluctuations) that is converted into heat is proportional to the dielectric-loss tangent $tg\,\delta_n\approx\omega_n\tau$ where $\omega_n\tau$ is the natural frequency of the dipole [8]. Accordingly, all other things being the same, formulas (26) and (30) imply that

$$\frac{1}{2}\omega_n\tau m r^2\left(\frac{\partial\varphi}{\partial t}\right)^2\approx\frac{1}{2}\xi_r r^2\left(\frac{\partial\varphi}{\partial t}\right)^2. \tag{56}$$

Hence, we obtain the estimate

$$\xi\sim\omega\tau m\sim10^{-33}.$$

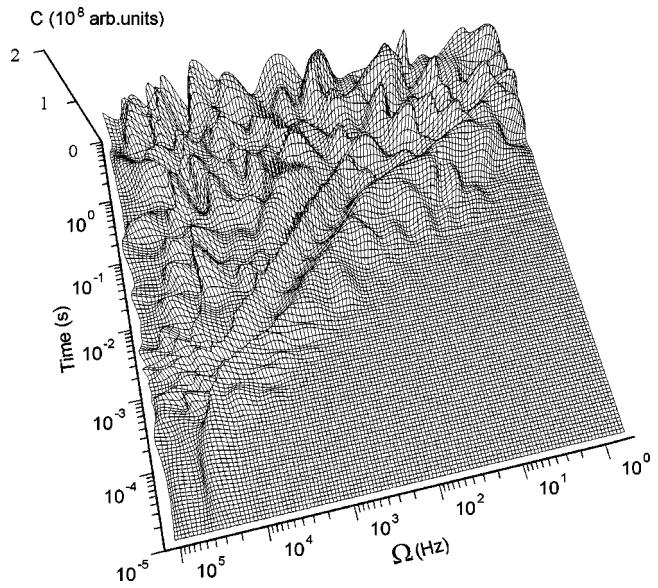

FIG. 2. Evolution of polarization-level spectrum under the action of an extremely weak harmonic ULF electric field.

IV. RESULTS

As is known, the disturbed SG equation has been solved analytically only in certain special cases [4,9]. Nevertheless, we will demonstrate that motion Eq. (49), which describes the transmission of signals in disperse systems with double electrical layers, allows resonancelike excitation at ULFs despite very stringent restrictions that were imposed on the equation. This section deals with the numerical analysis of Eq. (49) with a constraint on the length of the chain (the computational scheme is outlined in the Appendix). The analysis aims at ascertaining the nature of the excitation and to explore the possibilities for other effects.

As one would expect, the chain exhibits ULF ultrasensitivity in a wide range of relaxation times: $\tau_1\sim10^{-5}-10^0$ s. Figure 2 depicts the evolution of the polarization-level spectrum when the chain is subjected to an extremely weak harmonic electric field with a chain length l of 1 m and a field strength of $E=10^{-6}$ V/m. Numerical analysis was performed with the following realistic values of the parameters: $r=10^{-6}$ m, $a=2.1\times10^{-6}$ m, $\tau_1=1.6\times10^{-5}$ s, $c_o=10^5$, $\varepsilon_\infty=8$, $\varepsilon_s=650$, $\beta=1$, $\xi=10^{-33}$, and $m=1.6\times10^{-27}$ kg. Moreover, the values of ε_∞, ε_s, and τ_1 are typical of disperse systems where manifestations of ULF ultrasensitivity were first observed [1–3] according to our interpretation. The values of r and a are selected on the basis of [1–3]. In this study, unless otherwise stated, the term *polarization level*

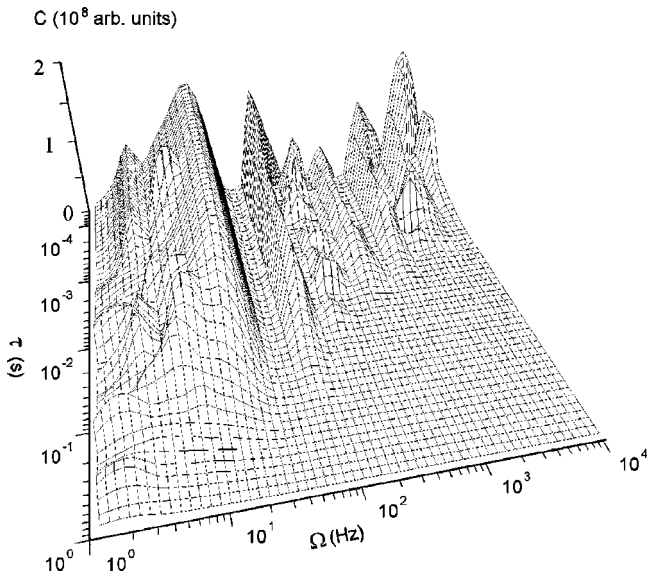

FIG. 3. Polarization level vs drive frequency and relaxation time.

means the number of elementary charges involved in polarization $c=Q/e$. This number is determined from a continuum version of formula (7), namely,

$$Q(x,t)=\beta\left\{V_1(x,t)+B(x,t)V_8(x,t)\frac{\partial\varphi}{\partial x}+B(x,t)V_9(x,t)\frac{\partial^2\varphi}{\partial x^2}\right\} \tag{57}$$

after the spectrum $\varphi_t(\Omega,t)$ has been computed.

Let us examine the behavior of the chain under the action of a ULF field. It can be seen that the polarization-level spectrum has a resonance-excitation portion if $t<1$ s. For $t>1$ s, this portion gradually changes into that of the dispersion law Debye characteristic. In the first stage, we observe main-resonance peaks and satellite resonances for $t>10^{-3}$ s. With $t\to 1$ s, they all shift to the region of $\Omega<10$ Hz. Such frequencies are called ultralow frequencies ULFs. The dispersion properties of the chain at ULFs become apparent if the Z axis is transformed to a logarithmic scale. In the final stage, the characteristic does not follow the Debye law in the strict sense. Instead, we can see a plateau disturbed at certain harmonics and occasionally disrupted by subharmonic bursts. Indeed, the evolution of the polarization-level spectrum depends on the parameters related to the driving, the oscillators, etc. Nevertheless, the pattern retains the distinctive features of Fig. 2 even when computed for other values of l and τ_1. Figure 3 shows this phenomenon in relation to the polarization level as a function of Ω and τ_1.

We note that a decrease in τ_1 corresponds to an increase in the temperature of the chain. It can be seen that the frequencies of both the main and the satellite resonances are virtually fixed when τ_1 is varied within a wide range: $\tau_1\sim 10^{-5}-10^{-2}$ s. A slight frequency shift occurs only when the chain is cooled in the region of $\tau>10^{-2}$ s. On the other hand, the region occupied by the satellite resonances extends to higher frequencies as the temperature is raised.

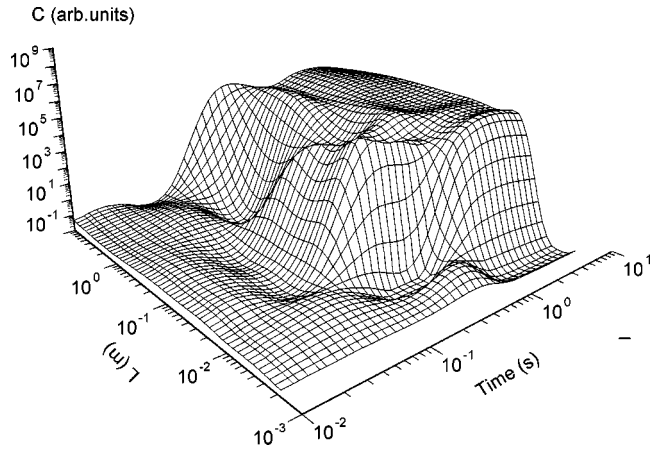

FIG. 4. Polarization level vs time and chain length for an extremely small drive amplitude.

Remarkably, in the realistic model under consideration, the chain exhibits the dependence of the polarization level on the chain length. Figure 4 illustrates how this size effect changes with time for $\Omega\sim 31$ Hz and E as low as 10^{-8} V/cm. In particular, the effect indicates that the chain may possess an ultrasensitivity to ULF. On the other hand, ultrasensitivity arises only if the chain length exceeds a certain threshold. Specifically, ultrasensitivity is impossible if l is smaller than 1 cm but is appreciable for $l\sim 5-10$ cm, with $r\sim 10^{-6}$ m and $a\sim 2.1\times 10^{-6}$ m (Fig. 4). In the latter case, the polarization level increases by a factor of 10^9. Furthermore, it was found that the polarization level of a long chain exposed to an extremely weak field may be as large as that of a short chain ($l<10^{-3}$ m) subjected to a strong field (Fig. 5). However, it takes a certain time for the response to develop after a harmonic field is applied with the delay increasing with η. The above behavior can be detected in spite of the considerable changes in the pattern when any of the parameters are varied.

The nonlinear nature of the above effects is demonstrated by Figs. 6(a) and 7. They show the polarization level [Fig. 6(a)] and phase velocity (Fig. 7) as functions of the coordinate and time. Figures 6(a) and 7 clearly shows that solitonlike excitations develop at both ends of the chain, with $l=1$ m and $t>0.2$ s. If $t<0.1$ s when the chain responds resonantly, then the polarization level oscillates fairly regularly throughout the chain exposed to an external field with $\Omega\sim 31$ Hz [Fig. 6(a)]. Afterward, these oscillations become more and more chaotic, starting from the chain ends. If $t>0.2$ s, the chaos gives way to distinct periodic positive bursts. This obviously suggests that solitonlike standing waves develop synchronously in the chain. Arising at the ends, they gradually extend to the entire chain. Clearly, any two neighboring dipoles occupied by any of the solitons oscillate in antiphase (since opposite charges of the dipoles prefer a positive-to-negative oscillation pattern). This growing oscillation seems to end in the rotation of the dipoles in opposite directions. The chain thus acquires a special type of dynamics whereby the charges of a dipole move throughout the sheath. Specifically, the rate of polarization bursts is

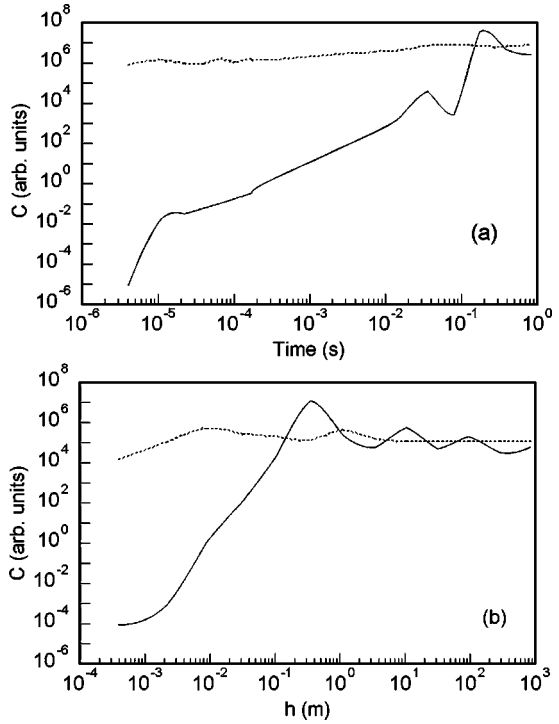

FIG. 5. Polarization level vs (a) time and (b) length for $\Omega \sim 31$ Hz. The solid and the dashed lines refer to $E=10^{-6}$ and 10^{5} V/m, respectively.

lower than the pump frequency by a factor of about 6 [Fig. 6(a)]. This is also confirmed by the power spectr in Fig. 6(b). For example, if the chain is subjected to an extremely weak harmonic field with $\Omega=31$ Hz, it exhibits polarization bursts at the fundamental frequency $f\sim 5$ Hz and its subharmonics $2f$ and $3f$. It was found that subharmonics at other frequencies may also appear and disappear as a result of bifurcations with respect to certain parameters.

V. DISCUSSION

It follows from the above results that a resonance response to a harmonic perturbation at any ULF develops during three to five periods. Afterward, the chain is in a chaotic state for three to seven periods (depending on parameters). Finally, its behavior changes to correspond to the Debye dispersion law. By this moment, the chain develops solitonlike wave packets, which are confined to its ends or occupy the entire chain. These features testify to the nonlinearity of the system dynamics, which obeys an SG-like equation. In simulating the oscillator coupling, the complicated and evidently nonlinear fashion in which the polarization level of any oscillator depends on those of its neighbors was taken into account, as well as the frequencies with which concentrated charges oscillate in them. The interaction between the oscillators was treated in the Coulomb approximation, allowing for the fact that the intercharge spacings vary with time. Indeed, if the parameters of the basic equations were varied, we could find many more trajectories, main and satellite resonances, and chaotic-region widths. Furthermore, we could observe domains in the distributions of the polarization level and sign throughout the chain. A deeper insight into the phenomena described by the model could be gained from its two-or three-dimensional versions. Also, quite a different pattern may be obtained if we allowed for the magnetic field of the oscillating dipoles. At higher driving frequencies, the magnetic field must scatter a fraction of the concentrated charges in the region where solitons are formed. This factor may reduce the polarization level at medium frequencies.

The size effect and ultrasensitivity in the chain are direct consequences of the strongly nonlinear coupling between the dipoles. Their moments change considerably, primarily due to the fact that c_1 varies from 0 to about $c_1 \approx c_o(\varepsilon_s-\varepsilon_\infty)$. In the context of this study, the maximum value of c_1 may be on the order of 10^{11}.

As indirect experimental evidence for our theoretical results, we cite the giant response of strongly compressed crystalline hydrates to an extremely weak electric field in the frequency range of 20–40 Hz [1–3]. This effect seems to cause the pronounced loss of mechanical strength (by a factor of 1.5–2) observed in some cases certain compressed crystal hydrates. Clearly, the ultrasensitivity spectrum of a substance can be determined from the dip in the ULF spectrum of the threshold of mechanical strength. The beauty of using this approach to design high-sensitivity ULF transducers consists in the following. We believe that ultrasensitivity is possible when crystalline hydrates experience short-term phase transitions involving partial dehydration produced by considerably nonuniform compression at a high pressure (over 5 kbar) or temperature [1–3]. Under such conditions, crystalline hydrates are basically heterogeneous media that can be regarded as one-dimensional seas of nonlinear electromagnetic oscillators (ideally, the oscillators can be regarded as grains with double electric layers). On the one hand, the short duration of the phase transitions allows one to ascertain the ultrasensitivity spectrum in the initial stage of excitation. On the other hand, we believe that the model furnished with realistic parameter values, such as those used above, can provide an estimate of the average dehydration time under highly nonuniform compression. The phase transition is sufficiently long for resonance electromagnetic excitation to develop with threshold parameter values allowing efficient detection of ULF ultrasensitivity from the mechanical response (impaired mechanical stability). If the threshold conditions of a pronounced response are aroused only by the moment when the state of the excited system entered the dispersion portion of the polarization characteristic, then supersensitivity would occur in the entire ULF region. Since the latter was never observed, we can infer that the oscillation ceased growing as early as the resonance stage. For systems with a narrow resonancelike peak, ULF ultrasensitivity is most likely to occur at $20<\Omega<40$ Hz, according to experiments [1–3]. Figure 2 demonstrates that this frequency range corresponds to an excitation time of about $t \sim 0.1-0.2$ s. Thus, we see that the attempts to attribute the ULF ultrasensitivity of the heterogeneous media (in the above-mentioned frequency range) to the Debye frequency dispersion only [1–3] were based on the highly overstated relaxation times for disperse systems ($\tau\sim 10^{-2}-10^{-1}$). The reason is that the early models relying on these values pre-

dict that ultrasensitivity peaks will lie fairly close to the ULFs at which the excitation threshold of the Bridgman effect decreases. In reality, experiments with certain model objects yield $\tau \sim 10^{-5}$ s at normal temperature [3]. Furthermore, the early models seem to be unable to adequately explain the shift of the ultrasensitivity spectral peak in the ULF region for crystalline hydrates under strong nonuniform compression, the effect of which was first reported in [2]. By contrast, the model suggested in this paper attributes the slight of the peaks to higher frequencies shift as the temperature of crystalline hydrates is raised to the fact that the delay is decreased below the threshold of electromagnetic spike as early as in the resonance stage. The numerical analysis showed that the decrease results neither from an increase in the number of elementary charges in the oscillators under heating nor from changes in the dissipation of oscillation energy, oscillator diameter, or spacing, etc. We believe that a shorter time of phase transitions in the crystalline hydrates under strong compression and heating leads to a shorter resonance-excitation time, which in turn produces the shift to higher frequencies.

It is worth noting that ultrasensitivity was also theoretically discovered in an overdamped Kramers oscillator subjected to a weak time-dependent signals with parametric noise [10]. Furthermore, high sensitivity to weak constant perturbation and noise was studied in the context of a chiral selective chemical reaction [11]. By contrast, the ultrasensitivity examined here is induced by a weak alternating signal and the response level depends on chain length, excitation time, and other parameters. However, the effect does not result from a radical change in the asymptotic behavior of the system (the crossover) in response to a noise-induced perturbation of a parameter appearing in the model equations. Instead, it is caused by nonlinear effects producing giant narrow peaks of charge density in the chain. Consequently, no crossover boundary conditions are required to test our model in experiments.

Finally, let us estimate the local electric field $E_{\rm int}$ between the sheaths of two neighboring oscillators. Existing for a limited period, the field arises when the dipoles intensely oscillate under local focusing during an electromagnetic spike. The formula $E=Q^2(4\pi\varepsilon\varepsilon_o\pi r^2 q_o)^{-1}$ yields $E_{\rm int} \sim 10^7-10^{11}$ V/cm, with the dipole charge Q set to its maximum value for the stated conditions, $Q\sim 10^{-12}-10^{-9}$ C. Such charge spikes can cause a microscopic breakdown at numerous sites together with shock waves and explosionlike phenomena. This effect is possible in various materials subjected to relatively weak ULF electric fields [1–3].

VI. CONCLUSION

We examined the behavior of a chain of closely spaced dipole oscillators ($a \geqslant 2r+\Delta$) with interrelated and variable dipole moments. To this end, a potential was determined for the dipoles. On the basis of this potential, the Euler-Lagrange equation was solved and a corresponding one-dimensional nonlinear-motion equation was derived. The latter was then transformed to a modified SG equation with dissipation.

The numerical analysis of the above equations suggests

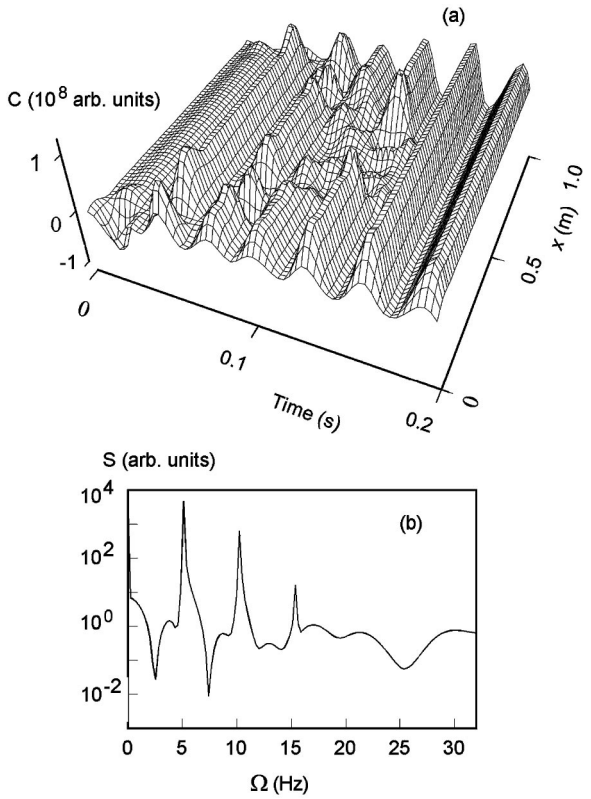

FIG. 6. (a) Polarization level vs time and the coordinate, and (b) the corresponding power spectrum after averaging over the chain. The data were obtained for an extremely small drive amplitude and $\Omega \sim 31$ Hz.

that the chain may feature strongly nonlinear dynamics. It was demonstrated that if a SLF harmonic field is applied to the chain, the latter first experiences a resonance type of excitation, then passes to chaos, and finally enters a state with the Debye dispersion. During the first stage, the resonance frequency shifts to still lower frequencies and may reach a fraction of a hertz. We also found some other interesting features typical of many systems with nonlinear cou-

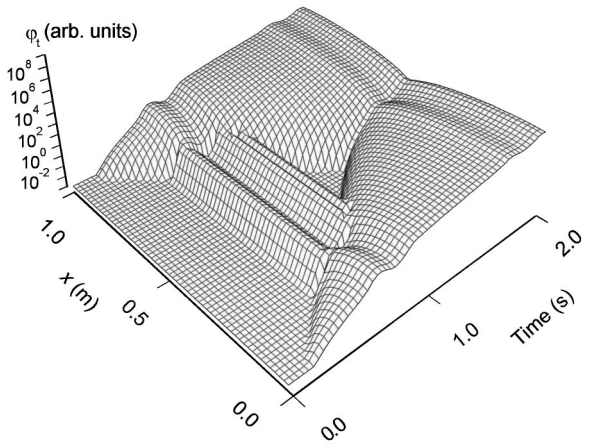

FIG. 7. Phase velocity vs time and the coordinates of the chain. The chain is driven at an extremely small field amplitude and $\Omega = 31$ Hz. The other parameter values are specified in the text.

pling, such as the emergence of resonance frequencies by heating in the first stage and the formation of solitonlike objects in the third one.

Remarkably, the computation has revealed the size effect in the chain. This implies that the model may possess ultrasensitivity to extremely weak periodic signals. We believe that such phenomena were observed in experiments with disperse substances exposed to a ULF electric field [1–3]. Apparently, experimental evidence for the size effect was the ultrasensitivity of crystalline hydrates in an appropriate disperse phase, with the particle size lying in the millimeter range [1–3]. With those media, ultrasensitivity arises if the amplitude of the perturbing signal is smaller than the electric-breakdown value by a factor of 1000.

Admittedly, we had to neglect many features of naturally occurring oscillator systems with variable dipole moments. Nevertheless, the paper has demonstrated some effects that were previously observed in physical experiments. We therefore believe that our approach can be used to predict phenomena.

ACKNOWLEDGMENTS

The author is grateful to T. V. Bakitskaya for his helpful participation in discussions.

APPENDIX

To numerically solve Eq. (49), we use an appropriate finite-difference method (see, e.g., [12,13]). Using the mesh function $\varphi_{n,i}=\varphi(nh,ik)$ for $\varphi(x,t)$, we obtain the following approximate formulas:

$$\varphi_t=(\varphi_{n,i+1}-\varphi_{n,i-1})/2k+O(k^2), \tag{A1}$$

$$\varphi_{tt}=(\varphi_{n,i+1}-2\varphi_{n,i}+\varphi_{n,i-1})/k^2+O(k^2), \tag{A2}$$

$$\varphi_{xx}=(\varphi_{n+1,i+1}-2\varphi_{n,i+1}+\varphi_{n-1,i+1}+\varphi_{n+1,i-1}-2\varphi_{n,i-1}+\varphi_{n-1,i-1})/2h^2+O(h^2+k^2). \tag{A3}$$

Inserting Eqs. (A1)–(A3) into Eq. (49) and neglecting the $O(k^2)$ and $O(h^2)$ terms, we arrive at

$$a_1(\varphi_{n+1,i+1}+\varphi_{n-1,i+1}+\varphi_{n+1,i-1}+\varphi_{n-1,i-1})+a_2\varphi_{n,i-1}+a_3\varphi_{n,i+1}+a_4\varphi_{n,i}=\Theta_o^2\sin(\varphi_{n,i})-\gamma, \tag{A4}$$

$$n=1,2,...,N; \quad i=0,1...I,$$

where

$$a_1=v_o^2/2h^2, \quad a_2=(\eta/2k-v_o^2/h^2+1/k^2),$$

$$a_3=(\eta/2k+v_o^2/h^2+1/k^2), \quad a_4=-2/k^2. \tag{A5}$$

Here, the parameters v_o, Θ_o, η, and γ are determined from Eqs. (50)–(53), respectively, with $x=nh$ and $t=ik$. The computational procedure for Eq. (A4) with $k=h$ is robust only if the step h is less than 0.1 [9]. If, e.g., $I\sim1000$ and $N\sim1000$ with $h\sim0.001$ m and $k=0.001$ s, then $l=Nh=1$ m and $t=Ik=1$ s, where l is the chain length and t is the observation time.

[1] E. G. Fateev, Dokl. Akad. Nauk **354**, 252 (1997) [Trans. Russ. Akad. Sci./Earth. Sci. Sect. **354**, 582 (1997)].
[2] E. G. Fateev, Pis'ma Zh. Eksp. Teor. Fiz. **65**, 876 (1997) [JETP Lett. **65**, 919 (1997)].
[3] E. G. Fateev, Zh. Tekh. Fiz. **66**, 93 (1996) [Tech. Phys. **41**, 571 (1996)].
[4] *Solitons in Action*, edited by K. Lonngren and A. Scott (Academic, New York, 1978).
[5] A. S. Davydov, *Solitons in Molecular* (Kluwer, Dordrecht, 1991).
[6] P. J. W. Debye, *Polar Molecules* (Chemical Catalog, New York, 1929).
[7] J. N. Israelachvili, *Intermolecular and Surface Forces* (Academic Press, New York, 1992).
[8] S. S. Dukhin, G. Kretzschmar, and R. Miller, *Dynamics of Adsorption at Liquid Interfaces* (Elsevier, Amsterdam, 1995).
[9] R. K. Dodd, J. C. Eilbeck, J. Gibbon, and H. C. Morris, *Solitons and Nonlinear Wave Equations* (Academic, New York, 1982).
[10] S. L. Ginzburg and M. A. Pustovoit, Phys. Rev. Lett. **80**, 4840 (1998).
[11] D. K. Kondepudi, I. Prigogine, and G. W. Nelson, Phys. Lett. A **111**, 29 (1985).
[12] W. F. Ames, *Numerical Methods for Partial Differential Equations* (Academic, New York, 1977).
[13] G. I. Marchuk, *Methods of Numerical Mathematics* (Springer-Verlag, New York, 1975).